

# Biexciton as a Feshbach resonance and Bose-Einstein condensation of paraexcitons in $\text{Cu}_2\text{O}$

Hoang Ngoc Cam

Institute of Physics, Vietnam Academy of Science and Technology,  
10 Dao Tan, Ba Dinh, Hanoi, Vietnam

November 6, 2018

Paraexcitons, the lowest energy exciton states in  $\text{Cu}_2\text{O}$ , have been considered a good system for realizing exciton Bose-Einstein condensation (BEC). The fact that their BEC has not been attained so far is attributed to a collision-induced loss, whose nature remains unclear. To understand collisional properties of cold paraexcitons governing their BEC, we perform here a microscopic consideration of the s-wave paraexciton-paraexciton scattering. We show its two-channel character with incoming paraexcitons coupled to a biexciton, which is a Feshbach resonance producing a paraexciton loss and a diminution of their background scattering length. The former elucidates the mechanism of the long-observed paraexciton loss, which turns out to be inefficient at temperatures near one Kelvin and below, whereas the latter makes the paraexciton scattering length in strain-induced traps negative under stress exceeding a critical value. Our rough estimates give this value of order of one kilobar, hence already moderate stress creates a serious obstacle to attaining a stable paraexciton BEC. Thus our results indicate that BEC of trapped paraexcitons might be achieved at a subkelvin temperature, but only under low stress.

## Introduction

Exciton in semiconductors is a Coulomb-bound pair of an electron in the conduction band and a hole in the valence band. In the low-density limit, excitons behave as bosons, so they may undergo Bose-Einstein condensation (BEC) if their lifetime is long enough to allow the system to reach quasiequilibrium.<sup>1–3</sup> Therefore BEC is expected in  $\text{Cu}_2\text{O}$  where the dipole-forbidden 1s excitons of the yellow series have relatively long lifetime. The state is split by the electron-hole exchange into the singlet paraexciton and higher lying triplet orthoexciton, separated by an energy of  $\Delta = 12$  meV.<sup>4</sup> The orthoexciton is quadruple allowed, while the paraexciton is strictly forbidden resulting in its particularly long lifetime.<sup>5</sup> Due to this property and yet to their large binding energy, paraexcitons in  $\text{Cu}_2\text{O}$  have long been considered a good system to realize exciton BEC in a three-dimensional solid.

Much effort has been made during the past several decades, but compelling evidence of BEC in  $\text{Cu}_2\text{O}$  has not been obtained.<sup>6–14</sup> It is believed, that the main obstacle is a collisional loss preventing paraexciton density from achieving the critical value for BEC.<sup>7,12–17</sup> The loss was also suggested to be the reason of the "explosion" observed by Gonokami's group when they were able

to realize the critical density for strain-confined paraexcitons at a subkelvin temperature.<sup>10</sup> It is conventionally attributed to Auger recombination, but its nature has not been elucidated.<sup>18</sup> Later, involvement of a biexciton<sup>19,20</sup> and inelastic collision of paraexcitons<sup>17</sup> have been suggested, but their microscopic mechanism is still open to make clear. In general, despite the recent experimental progress toward paraexciton BEC,<sup>10–13</sup> a basic theoretical issue of the problem – the interparticle interaction, remains unsolved.

To understand and possibly to control obstacles to paraexciton BEC, here we perform a microscopic consideration of the paraexciton-paraexciton scattering at low temperatures. We begin by formulating a Hamiltonian for the problem starting from its original electron-hole picture. This enables us to establish the interconversion between a pair of paraexcitons and that of orthoexcitons, which results in the two-channel character of the paraexciton scattering. To obtain salient features of the s-wave collision dominating scattering at low temperatures, we develop an approximate way of dealing with the nonlocal exchange part of interaction potentials in two channels, which is also the coupling potential. This makes it possible for us to estimate the paraexciton background scattering length, the binding energy of a biexciton supported by the closed channel as well as strength of the paraexciton-biexciton coupling. With this coupling the biexciton is not a bound state that can be detected, but a Feshbach resonance, which manifests itself through changes it makes to collisional properties of paraexcitons. Those include a paraexciton loss and an extra attractive interaction added to their background repulsive interaction. In strain-induced traps, wherein biexciton effects are enhanced with stress, the paraexciton scattering length turns negative as stress goes beyond a critical value  $S_0$ . Hence only stress not higher than  $S_0$ , which in our estimates is of order of one kilobar, can be used to create traps. This indicates that the explosion reported in ref. 10 is connected with the negative scattering length of strain-confined paraexcitons under moderate stress. Concerning the loss, with a linear dependence on the paraexciton-phonon scattering rate it can be made inefficient by lowering temperatures to the range near one Kelvin and below. Our results provide theoretical understanding of obstacles to paraexciton BEC, which offers interpretation of recent experimental results as well as suggests means to improve conditions for trapped paraexcitons to reach their BEC.

## Results

### Two-channel nature of paraexciton-paraexciton scattering

We use second quantization formalism for an elucidation of the effective spin-dependent two-body interaction among paraexcitons. We start from the fact, that excitons are long-live quasiparticles introduced for an effective description of electron-hole-pair systems with their inherent many-body Coulomb-mediated correlations. Each exciton is "dressed" by the Coulomb attraction of an electron with a hole and related to the other ones by the "residual" interaction that comes from the remaining part of the many-body correlations. Concerning the yellow-series 1s exciton in  $\text{Cu}_2\text{O}$  formed from double degenerate  $\Gamma_6^+$  and  $\Gamma_7^+$  bands, it splits into the triply degenerate orthoexciton  $\Gamma_5^+$  with spin  $J = 1$  and nondegenerate paraexciton  $\Gamma_2^+$  with  $J = 0$  according to the group-theoretical expansion

$$\Gamma_1^+ \otimes \Gamma_6^+ \otimes \Gamma_7^+ = \Gamma_2^+ \oplus \Gamma_5^+, \quad (1)$$

where the unit representation  $\Gamma_1^+$  characterizes symmetry of the  $1s$  hydrogenlike function describing the electron and hole relative motion in the exciton. From the relationship between basis functions of irreducible representations  $\Gamma_2^+$  and  $\Gamma_5^+$  and those of  $\Gamma_6^+$  and  $\Gamma_7^+$ , we have the momentum  $\mathbf{k}$  paraexciton state  $P_{\mathbf{k}}^+|0\rangle$  and that of orthoexcitons  $O_{M\mathbf{k}}^+|0\rangle$  ( $M = -1, 0, 1$  is the orthoexciton spin projection on the quantization axis) expressed as superpositions of correlated electron-hole pairs with total momentum  $\mathbf{k}$ .<sup>21</sup> With the aid of tables of Clebsch-Gordan coefficients relevant to irreducible representations of the  $O_h$  group,<sup>22</sup> we have

$$P_{\mathbf{k}}^+|0\rangle = \frac{1}{\sqrt{V}} \sum_{\mathbf{p}} F(\mathbf{p} - \beta\mathbf{k}) \frac{1}{\sqrt{2}} \left( e_{1/2, \mathbf{k}-\mathbf{p}}^+ h_{-1/2, \mathbf{p}}^+ + e_{-1/2, \mathbf{k}-\mathbf{p}}^+ h_{1/2, \mathbf{p}}^+ \right) |0\rangle, \quad (2)$$

$$O_{M\mathbf{k}}^+|0\rangle = \frac{1}{\sqrt{V}} \sum_{\mathbf{p}} F(\mathbf{p} - \beta\mathbf{k}) \times \begin{cases} e_{1/2, \mathbf{k}-\mathbf{p}}^+ h_{1/2, \mathbf{p}}^+ |0\rangle, & M = 1, \\ \frac{1}{\sqrt{2}} \left( e_{1/2, \mathbf{k}-\mathbf{p}}^+ h_{-1/2, \mathbf{p}}^+ - e_{-1/2, \mathbf{k}-\mathbf{p}}^+ h_{1/2, \mathbf{p}}^+ \right) |0\rangle, & M = 0, \\ e_{-1/2, \mathbf{k}-\mathbf{p}}^+ h_{-1/2, \mathbf{p}}^+ |0\rangle, & M = -1, \end{cases} \quad (3)$$

where  $|0\rangle$  is the semiconductor ground state and  $|0\rangle$  – that state mapped on the space of excitons,  $V$  – the sample volume,  $F(\mathbf{p} - \beta\mathbf{k})$  – the  $1s$  exciton envelope function in the momentum space with  $\beta = \mu_h/\mu_x$  the hole-to-exciton mass ratio,  $\mu_x = \mu_e + \mu_h$ . Taking into account the fact, that in relevant experiments only  $1s$  excitons are excited, we have the relationship between correlated electron-hole pairs and excitons inverse to equations (2) and (3),

$$\begin{aligned} e_{1/2, \mathbf{k}_e}^+ h_{1/2, \mathbf{k}_h}^+ |0\rangle &= \frac{1}{\sqrt{V}} F(\alpha\mathbf{k}_h - \beta\mathbf{k}_e) O_{1, \mathbf{k}_e + \mathbf{k}_h}^+ |0\rangle, \\ e_{1/2, \mathbf{k}_e}^+ h_{-1/2, \mathbf{k}_h}^+ |0\rangle &= \frac{1}{\sqrt{V}} F(\alpha\mathbf{k}_h - \beta\mathbf{k}_e) \left( P_{\mathbf{k}_e + \mathbf{k}_h}^+ + O_{0, \mathbf{k}_e + \mathbf{k}_h}^+ \right) |0\rangle, \\ e_{-1/2, \mathbf{k}_e}^+ h_{1/2, \mathbf{k}_h}^+ |0\rangle &= \frac{1}{\sqrt{V}} F(\alpha\mathbf{k}_h - \beta\mathbf{k}_e) \left( P_{\mathbf{k}_e + \mathbf{k}_h}^+ - O_{0, \mathbf{k}_e + \mathbf{k}_h}^+ \right) |0\rangle, \\ e_{-1/2, \mathbf{k}_e}^+ h_{-1/2, \mathbf{k}_h}^+ |0\rangle &= \frac{1}{\sqrt{V}} F(\alpha\mathbf{k}_h - \beta\mathbf{k}_e) O_{-1, \mathbf{k}_e + \mathbf{k}_h}^+ |0\rangle. \end{aligned} \quad (4)$$

Thus, according to equation (2) a paraexciton system in the electron-hole representation has the form of ensembles of zero-spin correlated electron-hole pairs of the type schematically shown in Fig. 1. The residual interaction among paraexcitons arises from correlations between the electron and hole of each pair with all the electrons and holes of the other pairs, which are governed by the Coulomb forces and Pauli exclusion principle of indistinguishability. It includes two-body, three-body, and so on interactions, among which in dilute conditions the two-body interaction dominates. There exist several ways of deriving an exciton Hamiltonian with two-body effective interaction from that of the original electron-hole system.<sup>23–26</sup> In our previous work<sup>27</sup> we have done this for the common case of direct-gap two-band semiconductors by adopting the bosonization approach of Hanamura<sup>23,24</sup> with the particles spin taken into consideration. In the same way, here we map the correlations among the constituents of two zero-spin correlated electron-hole pairs, which can be in three possible spin combinations as shown by three examples in Fig. 1, onto the

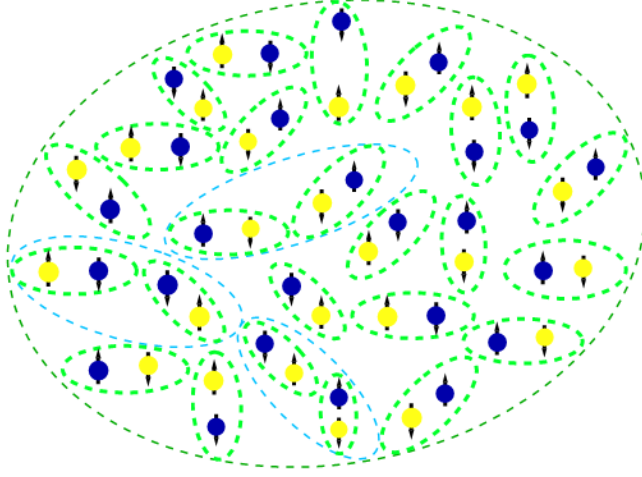


Figure 1: **Electron-hole representation of a system of paraexcitons.** Small blue (yellow) balls with arrows depict electrons (holes) with spin-up and spin-down. Dashed lightblue oval lines confine representative two-pair correlated structures.

exciton space to obtain the Hamiltonian

$$\begin{aligned}
H_{p-p} = & \sum_{\mathbf{k}} E_p(k) P_{\mathbf{k}}^+ P_{\mathbf{k}} + \sum_{\mathbf{k}} E_o(k) \sum_{M=-1,0,1} O_{M,\mathbf{k}}^+ O_{M,\mathbf{k}} \\
& + \frac{1}{2V} \sum_{\mathbf{k}_1, \mathbf{k}_2, \mathbf{q}} \left\{ U^d(q) O_{1, \mathbf{k}_1 + \mathbf{q}}^+ O_{-1, \mathbf{k}_2 - \mathbf{q}}^+ O_{-1, \mathbf{k}_2} O_{1, \mathbf{k}_1} \right. \\
& + \left[ U^d(q) + \frac{1}{2} U^{ex}(\mathbf{k}_1 - \mathbf{k}_2, \mathbf{q}) \right] \left[ P_{\mathbf{k}_1 + \mathbf{q}}^+ P_{\mathbf{k}_2 - \mathbf{q}}^+ P_{\mathbf{k}_2} P_{\mathbf{k}_1} + O_{0, \mathbf{k}_1 + \mathbf{q}}^+ O_{0, \mathbf{k}_2 - \mathbf{q}}^+ O_{0, \mathbf{k}_2} O_{0, \mathbf{k}_1} \right] \\
& - \frac{1}{2} U^{ex}(\mathbf{k}_1 - \mathbf{k}_2, \mathbf{q}) \left[ \left( O_{1, \mathbf{k}_1 + \mathbf{q}}^+ O_{-1, \mathbf{k}_2 - \mathbf{q}}^+ + O_{-1, \mathbf{k}_1 + \mathbf{q}}^+ O_{1, \mathbf{k}_2 - \mathbf{q}}^+ \right) O_{0, \mathbf{k}_2} O_{0, \mathbf{k}_1} + h.c. \right] \\
& + \frac{1}{2} U^{ex}(\mathbf{k}_1 - \mathbf{k}_2, \mathbf{q}) \left[ \left( O_{1, \mathbf{k}_1 + \mathbf{q}}^+ O_{-1, \mathbf{k}_2 - \mathbf{q}}^+ + O_{-1, \mathbf{k}_1 + \mathbf{q}}^+ O_{1, \mathbf{k}_2 - \mathbf{q}}^+ + O_{0, \mathbf{k}_1 + \mathbf{q}}^+ O_{0, \mathbf{k}_2 - \mathbf{q}}^+ \right) P_{\mathbf{k}_2} P_{\mathbf{k}_1} \right. \\
& \left. \left. + h.c. \right] \right\}, \tag{5}
\end{aligned}$$

where  $E_p(k)$  and  $E_o(k)$  denote respectively the paraexciton and orthoexciton energy,  $U^d$  and  $U^{ex}$  – energy densities of the direct and exchange exciton-exciton interaction, which are functionals of  $F$  depending parametrically on the mass ratios  $\beta$  and  $\alpha = 1 - \beta$ ,<sup>23,26</sup> and h.c. stands for hermitic conjugates. The last two terms in braces show, that the exchange interaction can flip the spin of interacting excitons. It either turns two longitudinal orthoexcitons ( $M = 0$ ) to a pair of transverse ones ( $M = 1, -1$ ) with opposite spins, or convert a paraexciton pair to a pair of orthoexcitons with zero total spin. Hereafter the term orthoexcitons will be used to refer exclusively to these ones. As  $U^{ex} > 0$ , we see that the two-boby interaction among paraexcitons is generally repulsive except for the case of the exchange interaction between two orthoexcitons, which is attractive. Mechanism of the exchange interaction is schematically shown on an example in Fig. 2.

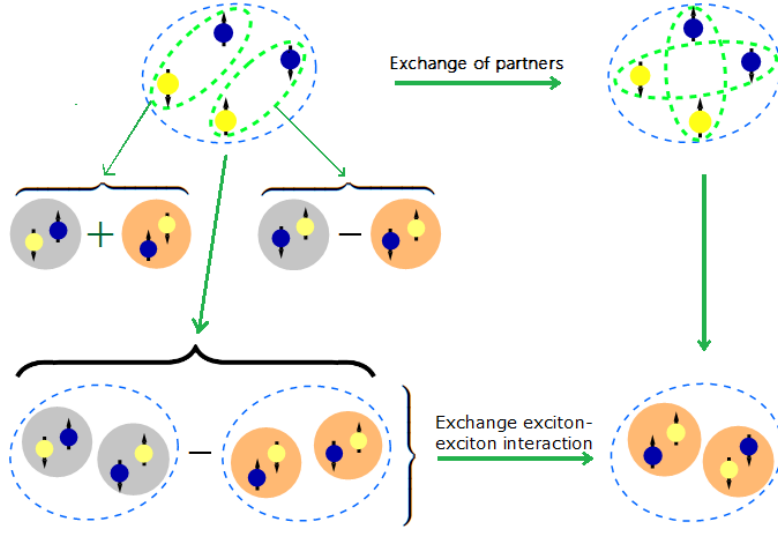


Figure 2: **Mechanism of the exchange exciton-exciton interaction.** Grey (orange) balls denote the dark paraexciton (bright orthoexcitons) with the spin projection equal to the sum of those of the constituent electron and hole. Left: On the top is one of complexes of two correlated electron-hole pairs which constitute two correlated paraexcitons. The complex includes two electrons (two holes) with opposite spins. Each correlated pair is represented in the exciton space by a linear combination of a paraexciton and a longitudinal orthoexciton in accordance with equation (4). As a result, the whole complex is represented by a combination of one correlated pair of paraexcitons and that of longitudinal orthoexcitons. Right: The electron-hole complex on the top is obtained from the one on the left by an exchange of partners between two pairs. It is represented in the exciton space by a pair of correlated transverse orthoexcitons with opposite spin directions. Thus, the exchange correlations between two electron-hole pairs are reproduced in the exciton space by the exchange exciton-exciton interaction.

Thus, with the effective two-body interaction taken into consideration, a "paraexciton system" incorporates not only paraexcitons, but also orthoexcitons that go in pairs. In this connection, neither paraexciton pairs nor orthoexciton ones can form eigenstates of Hamiltonian (5). They form just components, or substates of eigenstates, which have the form of two-exciton vectors with definite momentum

$$\Psi_{p-p}(\mathbf{K}) = \frac{1}{\sqrt{2V}} \sum_{\mathbf{s}} \left[ \psi_{pp}(\mathbf{s}) P_{\mathbf{s}+\mathbf{K}/2}^+ P_{-\mathbf{s}+\mathbf{K}/2}^+ + \frac{1}{\sqrt{3}} \psi_{po}(\mathbf{s}) \left( O_{0,\mathbf{s}+\mathbf{K}/2}^+ O_{0,-\mathbf{s}+\mathbf{K}/2}^+ \right. \right. \\ \left. \left. O_{-1,\mathbf{s}+\mathbf{K}/2}^+ O_{1,-\mathbf{s}+\mathbf{K}/2}^+ + O_{1,\mathbf{s}+\mathbf{K}/2}^+ O_{-1,-\mathbf{s}+\mathbf{K}/2}^+ \right) \right] |0\rangle, \quad (6)$$

where  $\psi_{pp}$  and  $\psi_{po}$  are envelope functions respectively of "bare" paraexciton and orthoexciton pairs. The Schrodinger equation  $H_{p-p}\Psi_{p-p}(\mathbf{K}) = E_{p-p}(k)\Psi_{p-p}(\mathbf{K})$  leads to a system of equations

for  $\psi_{pp}$  and  $\psi_{po}$ ,

$$\begin{aligned}
& - \left( \frac{\hbar^2 s^2}{\mu_x} + E \right) \psi_{pp}(\mathbf{s}) + \frac{1}{V} \sum_{\mathbf{q}} \left[ U^d(\mathbf{q}) + \frac{1}{2} U^{ex}(2\mathbf{s}, \mathbf{q}) \right] \psi_{pp}(\mathbf{s} + \mathbf{q}) \\
& \quad + \frac{\sqrt{3}}{2V} \sum_{\mathbf{q}} U^{ex}(2\mathbf{s}, \mathbf{q}) \psi_{po}(\mathbf{s} + \mathbf{q}) = 0, \\
& \left( -\frac{\hbar^2 s^2}{\mu_x} + 2\Delta - E \right) \psi_{po}(\mathbf{s}) + \frac{1}{V} \sum_{\mathbf{q}} \left[ U^d(\mathbf{q}) - \frac{1}{2} U^{ex}(2\mathbf{s}, \mathbf{q}) \right] \psi_{po}(\mathbf{s} + \mathbf{q}) \\
& \quad + \frac{\sqrt{3}}{2V} \sum_{\mathbf{q}} U^{ex}(2\mathbf{s}, \mathbf{q}) \psi_{pp}(\mathbf{s} + \mathbf{q}) = 0, \tag{7}
\end{aligned}$$

where  $\mu_x$  is assumed the same for both types of the exciton,  $E = k_B T$  ( $k_B$  is the Boltzmann constant,  $T$  – the temperature) is paraexciton thermal energy with their scattering threshold chosen as the energy zero. These equations describe two-channel paraexciton-paraexciton scattering, wherein the open (background) channel of incoming paraexcitons is coupled by the exchange interaction potential to the closed channel formed by the interaction potential between two orthoexcitons having energy higher than the paraexciton threshold energy by amount  $2\Delta$ . Hereafter we confine ourselves to the s-wave scattering at such low temperatures, that  $E \ll 2\Delta$  and the rate of para-ortho up-conversion is practically zero. In that case we can describe the scattering in the first approximation by two uncoupled channels and take their coupling into consideration in the next approximation.

### Approximate interaction potentials and solutions for bare channels

To proceed, we need to define interaction potentials in bare channels. Their direct part is known,<sup>28</sup> but we face the challenge of describing the exchange part. As expected in the case, when real interactions in a many-particle system are described in terms of an effective interaction between quasiparticles, the exchange exciton-exciton interaction is nonlocal. From a presentation for  $U^{ex}$  (see Supplementary Information (SI)) we observe, that the degree of its nonlocality decreases with decrease of  $\beta$  – the small mass ratio, disappearing in the limit  $\beta \rightarrow 0$ , when it equals the exchange energy in Heitler-London theory of the hydrogen molecule.<sup>29,30</sup> This suggests, that the expansion of  $U^{ex}$  into a series of powers of  $\beta$  might provide a useful approximation to the exchange interaction potential,

$$\begin{aligned}
& \frac{1}{2V} \sum_{\mathbf{q}} U^{ex}(2\mathbf{s}, \mathbf{q}) \psi(\mathbf{s} + \mathbf{q}) = \int \exp[i\mathbf{s}\mathbf{r}] d^3r \\
& \times \left[ A_0(r) + \beta A_1(r) \frac{d}{dr} + \beta^2 A_2(r) \frac{d^2}{dr^2} + \beta^3 A_3(r) \frac{d^3}{dr^3} + \dots \right] \phi(r) \equiv \int \exp[i\mathbf{s}\mathbf{r}] d^3r \mathcal{V}^{ex}(r) \phi(r), \tag{8}
\end{aligned}$$

if appropriately truncated. Here  $\phi$  is any of s-wave functions of bare channels in real space, and functions  $A_0(r), A_1(r), \dots$  depend parametrically on  $\beta$  falling off exponentially at large distances. The truncation order depends on  $\beta$  value, which cannot be acquired from the band extremum value

of electron and hole masses. Because of the exciton considerable spread in momentum space<sup>31</sup> and nonparabolicity of the valence band,<sup>32</sup> both  $\mu_h$  and  $\mu_x$  depend on the wave vector. We take the averaged value of  $\beta$  following from the ratio  $\mu_r/\mu_x = (1 - \beta)\beta$  with reduced mass  $\mu_r$  drawn from the relation  $E_b a_x^2 = \hbar^2/2\mu_r$  ( $E_b$  and  $a_x$  are the exciton binding energy and effective radius, respectively). Thus, to a set of values of the key parameters  $E_b$ ,  $a_x$ , and  $\mu_x$ , there corresponds a value of  $\beta$  determining interaction potentials. Let us take the commonly accepted values  $a_x = 0.7$  nm,  $E_b = 150$  meV and  $\mu_x = 2.6m_0$  ( $m_0$  is the free electron mass), then  $\beta \approx 0.28$ . For this value we can truncate expansion (8) at the third term, and as a result, equations for the  $\chi$ -function ( $\chi = r\phi/4\pi$ ) of the background s-wave scattering and possible biexciton read

$$2(\beta - 1)\beta E_b \chi_E'' + [\mathcal{U}^d(x) + F_0(x) - E] \chi_E + \beta F_1(x) \chi_E' + \beta^2 F_2(x) \chi_E'' + \beta^3 F_3(x) \chi_E''' = 0, \quad (9)$$

$$2(\beta - 1)\beta E_b \chi_b'' + [\mathcal{U}^d(x) - F_0(x) + 2\Delta - E_0] \chi_b - \beta F_1(x) \chi_b' - \beta^2 F_2(x) \chi_b'' - \beta^3 F_3(x) \chi_b''' = 0, \quad (10)$$

with  $E_0$  the biexciton energy,  $x \equiv r/a_x$  and functions  $F_0, F_1, F_2, F_3$  are expressed in terms of functions  $A_0, A_1, A_2, A_3$  (see SI). A change in deciding on a particular value for a key parameter entails quantitative changes in solutions for bare channels as well as their coupling, but the qualitative picture of the paraexciton scattering remains the same as presented below for  $\beta = 0.28$ .

Numerical solution of equation (9) for  $E = 0$  gives function  $\chi_0$ , whose plot's intersection with the  $x$ -axis gives the background scattering length  $a_{bg} \approx 1.45a_x$ . This result is considerably smaller than our rough hard-core estimate<sup>28</sup> and that computed by quantum Monte Carlo method for  $\beta = \alpha$ .<sup>33</sup> The quantity determines solely the background phase shift  $\delta_{bg}$  of slow paraexcitons.<sup>21</sup> Condition for paraexcitons to be slow depends on the range of paraexciton-paraexciton interaction potential  $\mathcal{V}_{bg} = \mathcal{U}^d + \mathcal{V}^{ex}$ , which in its turn is defined by functions  $\mathcal{U}^d(x)$  and  $F_0(x), \dots, F_3(x)$ . We get the range about  $3.5a_x$ , thus paraexcitons having  $k \ll (3.5a_x)^{-1} \approx 0.4 \text{ nm}^{-1}$  are slow. To be specific, we set the point  $T = 1.2 \text{ K}$  corresponding to  $k \approx 0.06 \text{ nm}^{-1}$  the upper bound of the slow paraexcitons range. As to equation (10), we find by the customary variational procedure, that it has one bound state – the biexciton with binding energy  $\mathcal{E}_b = 2\Delta - E_0 \approx 12.78 \text{ meV}$  and the corresponding wave function

$$\chi_b = 1.22267 x \exp[-1.8 \exp(-2.475 x)] [\exp(-2.48 x)]^{0.279}. \quad (11)$$

The obtained value for  $\mathcal{E}_b$  is much larger than the result of Brinkman et al.<sup>34</sup> and almost coincides with that of Huang.<sup>35</sup>

To have an idea of the shape of potentials  $\mathcal{V}_{bg}$  and  $\mathcal{V}_{cl} = \mathcal{U}^d - \mathcal{V}^{ex}$ , we perform localization procedures to obtain their approximate local equivalents.<sup>36</sup> Neglecting for simplicity small  $\beta^3$ -terms in equations (9) and (10), we turn them into usual Schrodinger equations by transformations  $\chi_E(x) = T_E(x)\Phi_E(x)$  and  $\chi_b(x) = T_b(x)\Phi_b(x)$ , respectively. The acquired energy-dependent local potentials  $V_{bg}$  and  $V_{cl}$  are shown in Fig. 3.

## Effects of biexciton as a Feshbach resonance

The coupling of two channels, when it is "turned on", induces oscillations between paraexciton scattering states and the biexciton, which is no longer a bound state, but just a quasistationary state,<sup>21</sup> or a scattering resonance<sup>37</sup> with an energy uncertainty  $\Gamma_c$  and the corresponding lifetime

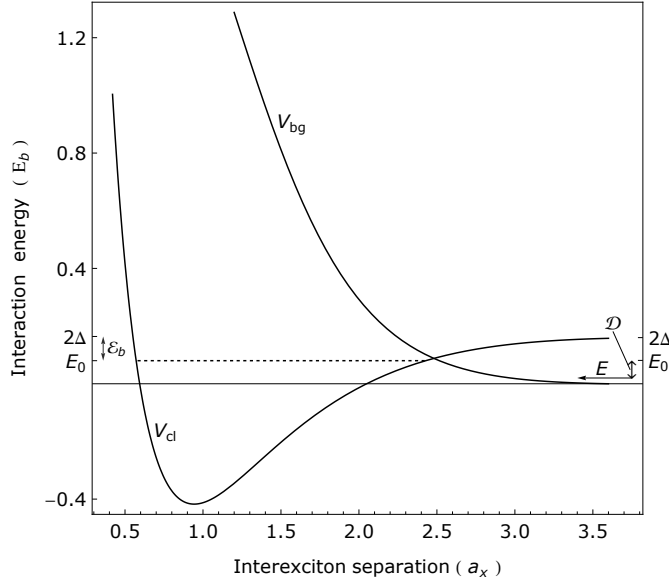


Figure 3: **Approximate local equivalents of interaction potentials in bare channels.**  $V_{bg}$  is presented for  $E = 0$ , whereas  $V_{cl}$  – for  $E = E_0$ . Their shape resembles that of the interaction potential between hydrogen atoms respectively in their singlet and triplet molecular states.<sup>21</sup> For actual interexciton distances the interaction between paraexcitons in the open channel is repulsive, whereas that between orthoexcitons in the closed channel is attractive. With zero of energy chosen at the paraexciton scattering threshold, the interaction potential between orthoexcitons is shifted upward by the energy of  $2\Delta$  involving the biexciton energy (dotted line) to be "embedded" in the scattering continuum.

$\tau = \hbar/\Gamma_c$ . This explains the fact why biexciton has not been detected in  $\text{Cu}_2\text{O}$ . In quantum-mechanical scattering theory, the resonance width, which is called also the coupling strength, is obtained from the second-order correction to the discrete energy level caused by perturbation in the form of the coupling potential.<sup>21,37</sup> In our case,  $\Gamma_c \propto \int \sqrt{E} dE [\langle \phi_E | \mathcal{V}^{ex} | \phi_b \rangle]^2 \delta(E - E_0) = \sqrt{E_0} [\langle \phi_{E_0} | \mathcal{V}^{ex} | \phi_b \rangle]^2$ . To get the transition matrix element, we solve equations (7) in the real space for  $\phi_{pp} = \phi_{E_0}$  and  $\phi_{po} = \phi_b$  with the approximate  $\mathcal{V}^{ex}$ , taking into account the fact that  $\phi_b = 4\pi\chi_b/r$  is the solution of equation (10). Computations give  $\Gamma_c \approx 7.85$  meV, which is of the same order as the biexciton binding energy. Resonance scattering of paraexcitons happens when their energy matches the interval of width  $\Gamma_c$  around  $E_0$  through the mechanism illustrated in Fig. 4. Such a phenomenon is long known in nuclear physics as a Feshbach resonance.<sup>38</sup> They have lately become an important experimental tool for controlling properties of cold atomic gases.<sup>39</sup> In comparison with magnetic Feshbach resonances in the last, the quasibiexciton in  $\text{Cu}_2\text{O}$  has two distinctive features. First, its strong coupling with the open channel by the exchange exciton-exciton interaction potential, which is at once the ruling part of interaction potentials in bare channels. In this connection the resonance effects hold over a wide off-resonance area, in contrast to atomic gases, where they take place in a narrow resonance area. Second, the quasibiexciton is a decaying state by itself having a width  $\Gamma_{qb}$  connected with all damping mechanisms – partly a consequence



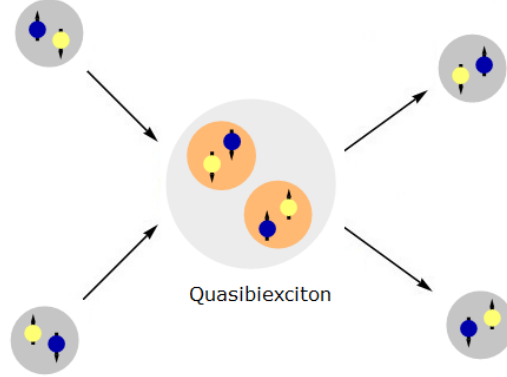


Figure 4: **Resonance scattering of paraexcitons on the quasibiexciton.** Two incoming paraexcitons encounter, interact via spin-flip exchange interaction potential and convert to an orthoexciton pair, which attracts each other forming temporarily the quasibiexciton. After the time  $\tau$  elapses, two orthoexcitons convert to a pair of paraexcitons leading to the quasibiexciton decay.

of that, the system under consideration is not quite closed, but coupled to surroundings.

Mixing of paraexcitons with the quasibiexciton as a decaying resonance gives rise to a resonance factor in their s-wave scattering matrix element,<sup>21,37</sup>

$$S_0 = \exp[2i\delta_{bg}] \left[ 1 + i \frac{\Gamma_c}{\mathcal{D} - i(\Gamma_c + \Gamma_{qb})/2} \right], \quad (12)$$

where  $\mathcal{D}$  is the detuning of scattering energy from the resonance,  $\mathcal{D} = 2\Delta - \mathcal{E}_b - E$  (see Fig. 3). From here we have the total s-wave scattering cross section  $\sigma_t = 2\pi(1 - \text{Re}S_0)/k^2$ ,

$$\sigma_t = \frac{\pi}{k^2} \left[ 4\sin^2 \delta_{bg} + \frac{\Gamma_c(\Gamma_c + \Gamma_{qb})}{\mathcal{D}^2 + (\Gamma_c/2 + \Gamma_{qb}/2)^2} \cos(2\delta_{bg}) + 2 \frac{\mathcal{D}\Gamma_c}{\mathcal{D}^2 + (\Gamma_c/2 + \Gamma_{qb}/2)^2} \sin 2\delta_{bg} \right]. \quad (13)$$

As seen, coupling to the quasibiexciton causes a resonance scattering superimposed on the paraexciton background scattering. This is described by the second and last terms in brackets presenting respectively the resonance scattering and its interference with background scattering. They include two quasibiexciton effects. First, a paraexciton loss connected with an inelastic component in the resonance scattering, whose rate  $A = v\sigma_r$  ( $v$  is the mean velocity of the particle undergoing scattering) is defined by the inelastic cross section  $\sigma_r = \pi(1 - |S_0|^2)/k^2$ ,

$$A = 4\pi \frac{\hbar^2}{\mu_x} \sqrt{\frac{6}{\mu_x E}} \frac{(\Gamma_c/2)(\Gamma_{qb}/2)}{\mathcal{D}^2 + (\Gamma_c/2 + \Gamma_{qb}/2)^2}. \quad (14)$$

Second, a change in the paraexciton-paraexciton interaction described by the elastic cross section  $\sigma_e = \sigma_t - \sigma_r$ . Obviously, the terms other than  $4\sin^2 \delta_{bg}$  in  $\sigma_e$  together represent an additional interaction joining up with the background paraexciton-paraexciton interaction. Rich physics of resonance effects, whose scale is defined by the relation between the quasibiexciton total width

and detuning, is beyond the scope of this paper. Here we consider them in the off-resonance area, where  $(\Gamma_c/2 + \Gamma_{qb}/2)/\mathcal{D} < 1$ , which is pertinent to conditions of recent experiments. Then, being of  $(\Gamma_c/2\mathcal{D})^2$  scale, the resonance term in  $\sigma_e$  is relatively small. Hence we have for slow paraexcitons,

$$\sigma_e|_{ka_{bg} < 1} \approx 4\pi \left\{ a_{bg} - \frac{1}{k} \frac{\Gamma_c}{2\mathcal{D}} \left[ 1 + \left( \frac{\Gamma_c}{2\mathcal{D}} + \frac{\Gamma_{qb}}{2\mathcal{D}} \right)^2 \right]^{-1} \right\}^2. \quad (15)$$

Thus, coupling to the quasibiexciton gives rise to an attractive interaction characterized by the term  $a_{res} \propto -\Gamma_c/2\mathcal{D}$  in the paraexciton scattering length  $a = a_{bg} + a_{res}$ . Regarding  $A$ , along with  $\Gamma_c/2\mathcal{D}$ , it is proportional to the ratio  $\Gamma_{qb}/2\mathcal{D}$ . Let us assume, that the quasibiexciton decay width is about two times that of paraexcitons,  $\Gamma_{qb}/2 \approx \Gamma_p$ . Besides a negligibly small population relaxation rate,  $\Gamma_p$  comprises homogeneous broadening due to the exciton-exciton and exciton-phonon scattering,  $\Gamma_{x-x}$  and  $\Gamma_{ph}$ , and inhomogeneous broadening  $\Gamma_{inh}$  due to fluctuations of the sample structure and applied fields. Consequently, the loss rate depends on the density, temperature, sample quality as well as inhomogeneity of external fields over the sample. We see, that  $\Gamma_{ph}$  makes the loss persistent at low densities<sup>7,17</sup> and  $\Gamma_{inh}$  is a source of uncertainty causing measurements of the loss rate diverge.<sup>14</sup>

## Quantitative estimates and interpretation of recent experimental results

We limit our rough estimates to scattering of slow paraexcitons in harmonic traps induced by moderate uniaxial stress – conditions covering those of recent experiments on BEC in  $\text{Cu}_2\text{O}$ .<sup>10–13</sup> Such traps are necessary to avoid paraexciton heating and diffusion as well as to lower the critical density.<sup>7,12</sup> By reducing  $\Delta$ ,<sup>40,41</sup> stress moves the quasibiexciton position downwards the scattering threshold (see Fig. 3). Coupling of scattering states to a resonance close to the threshold is energy-dependent. As a consequence, one has to replace the coupling strength  $\Gamma_c$  in equations (12) – (15) by the function  $\gamma_r(E) = \Gamma_c \sqrt{E} / (E_0^2 + \Gamma_c^2/4)^{1/4}$ .<sup>21</sup> From stress dependence of  $\Delta$  we find that the off-resonance condition corresponds to the applied stress  $S \lesssim 2$  kbar. At  $T \leq 1.2$  K  $\gamma_r(E)/\mathcal{D}$  is small and  $\Gamma_p/\mathcal{D}$  – negligibly small (we see later that  $\Gamma_p$  is at most several microelectronvolt). Accordingly, equations (14) and (15) give the measure of quasibiexciton effects in the approximate form

$$a_{res} \propto -\sqrt{\frac{\hbar^2}{\mu_x}} \frac{\Gamma_c}{2\mathcal{D}}, \quad A \propto \frac{\hbar^2}{\mu_x} \frac{\Gamma_c}{2\mathcal{D}} \frac{\Gamma_p}{\mathcal{D}}, \quad (16)$$

showing, that  $a$ , and with it the elastic collision rate  $K = \sigma_e v \propto a^2$ , are independent of  $\Gamma_p$ . On contrast, the loss rate  $A \propto \Gamma_p$ , which at low densities and small inhomogeneity equals  $\Gamma_{ph}$ . Because interaction of excitons with longitudinal acoustic phonons is stress-independent and that with transverse acoustic ones is weak,<sup>42</sup> we assume the value of  $\Gamma_{ph}$  at 1.2 K under moderate stress to be the same 80 neV as measured under zero stress.<sup>43</sup> Neglecting in the following inhomogeneity of the strain field, we put  $\Gamma_p \simeq \Gamma_{x-x} + \Gamma_{ph}$  with  $\Gamma_{x-x} = \hbar n (A + K)$  computed by iterations and obtain  $A$  for different  $S$  at a particular density. Along with  $a$ , which decreases with increasing  $S$  (see Fig. 5a), these parameters are sensitive to  $S$  (see Fig. 5b & 5c). Including a term proportional to  $a^2$ , they have a minimum at  $S_0$ , where  $a = 0$ , then begin to rise gaining steep increase when stress approaches 2 kbar, which is close to the resonance area of  $\Gamma_c/2\mathcal{D} \gtrsim 1$ . Actually, the increase

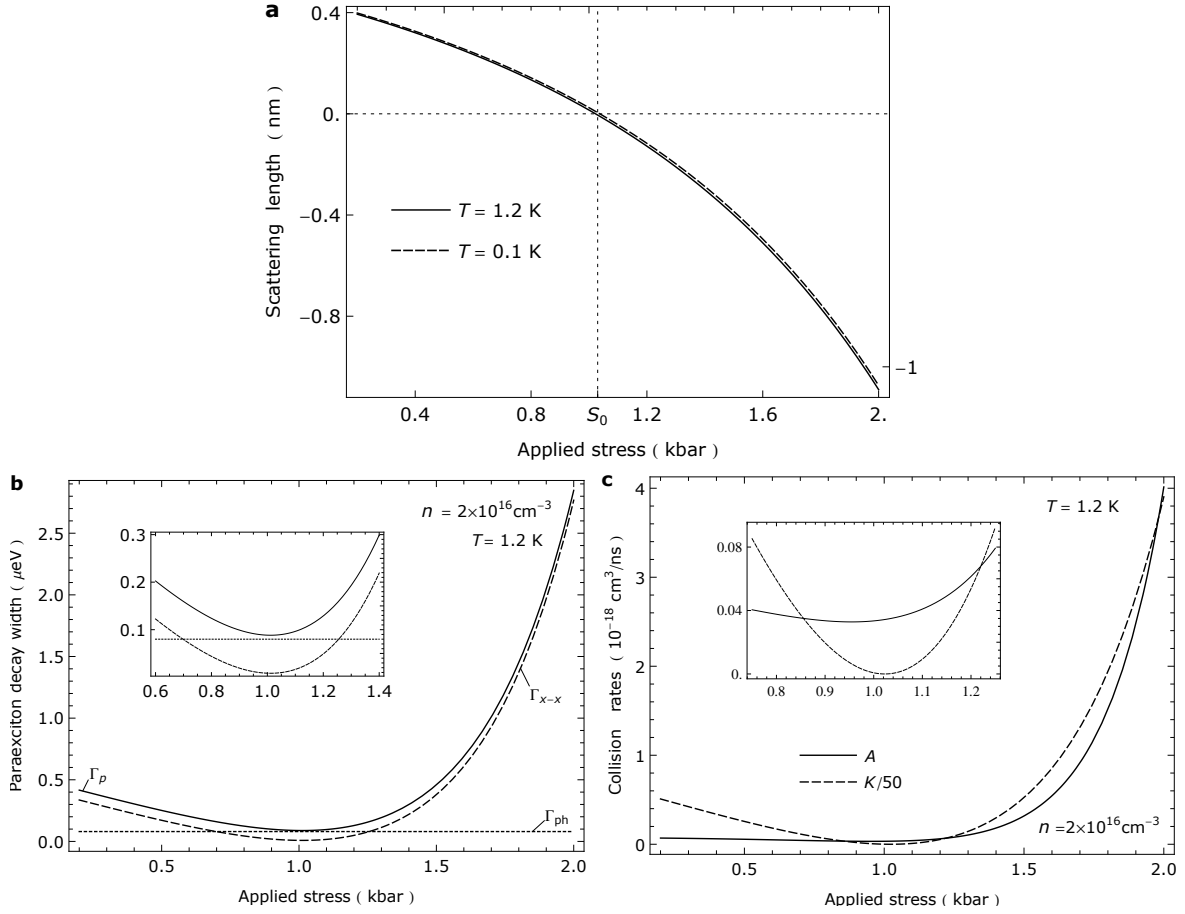


Figure 5: **Stress dependence of the parameters describing quasibiexciton effects on scattering of slow paraexcitons.** (a) Scattering length decreases monotonically with the applied stress changing its sign at  $S_0 \approx 1$  kbar, then rapidly gains considerable negative values: under  $S = 2$  kbar,  $|a| \approx 1.1 \text{ nm} > a_{bg}$ . The results depend little on the temperature. (b) Paraexciton decay width and its two components in the absence of inhomogeneous broadening. Being nearly proportional to  $a^2$ , at small values of the applied stress  $\Gamma_{x-x}$  decreases moderately taking its minimum at  $S_0$ , then rises speeding up when  $S$  approaches 2 kbar. So does  $\Gamma_p$ , which differs from  $\Gamma_{x-x}$  by the small constant  $\Gamma_{ph}$ . The relationship between  $\Gamma_p$ ,  $\Gamma_{x-x}$  and  $\Gamma_{ph}$  in the interval round 1 kbar is shown magnified in the inset. (c) Paraexciton loss rate on the background of the fiftyfold reduced elastic collision rate  $K$ . The behaviour of  $K$  is almost the same as  $\Gamma_{x-x}$ , but unlike the latter, it does not depend on the density. As to  $A$ , it varies slightly in the range before 1.1 kbar, but after the point grows steeply due to both increase of  $\Gamma_p$  and decrease of  $\mathcal{D}$  (see equation (15)). The inset shows the relationship between  $A$  and reduced  $K$  in the vicinity of their minimum.

of  $A$  with stress has been observed at moderate and high stress values.<sup>16</sup> Figure 5b shows, that apart from an interval around  $S_0$ , where  $\Gamma_{ph} > \Gamma_{x-x}$ , in general under stress the paraexciton

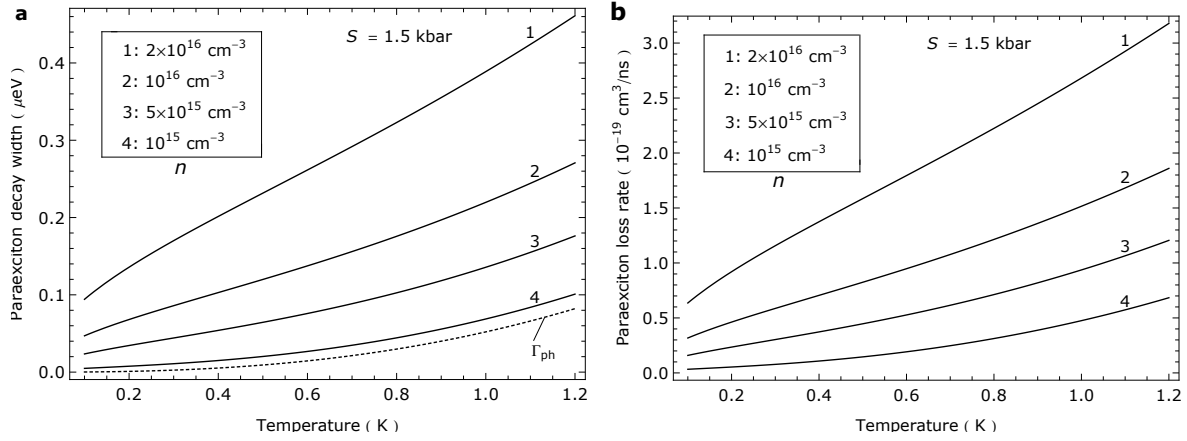


Figure 6: **Temperature dependence of parameters characterizing the decay and loss of slow paraexcitons at different densities.** (a) Paraexciton decay width varying with temperature under applied stress of 1.5 kbar as  $\Gamma_p \simeq (0.052T^{5/2} + 0.015nT^{1/2}) \mu\text{eV/K}$  ( $n$  – density measured in  $10^{15} \text{ cm}^{-3}$ ). The exciton-exciton scattering contributes to the decay already at a density as low as  $10^{15} \text{ cm}^{-3}$ . (b) Paraexciton loss rate decreasing with temperature nearly in the same way, as its decay width. For the density  $2 \times 10^{16} \text{ cm}^{-3}$  realized in today's standard experiments, the loss rate falls off threefold when temperature drops from 1.2 K to 0.2 K.

decay is governed by exciton-exciton scattering. Concerning the elastic and inelastic collision rates, the former absolutely dominates with the ratio  $K/A$  ranging from about 20 near  $S_0$  to over 50 away from the point (see Fig. 5c). The factor is favorable for evaporative cooling of thermal paraexciton clouds.<sup>44</sup> The domination holds with decreasing temperature, because  $K \propto T^{1/2}$  and  $A$  drops slightly faster. In fact, as seen from Fig. 5b, for  $S \approx 1$  kbar,  $\Gamma_{ph} \simeq \Gamma_p$ , so we get from temperature dependence of paraexciton mobility under  $S = 1$  kbar  $\Gamma_{ph}(T) \propto T^{5/2}$ .<sup>41</sup> As to  $\Gamma_{x-x}$ , for densities up to  $10^{17} \text{ cm}^{-3}$ ,  $\Gamma_{x-x} \simeq \hbar n K \propto nT^{1/2}$ . Thus  $A \propto \Gamma_p = (c_1 nT^{1/2} + c_2 T^{5/2})$ , where  $c_1, c_2$  – constants. The two parameters are plotted against temperature in Fig. 6. Figure 6a indicates another time, that under an applied stress outside vicinity of  $S_0$ , the exciton-exciton elastic scattering plays the leading part in paraexciton decay down to  $n = 5 \times 10^{15} \text{ cm}^{-3}$ . At  $n = 2 \times 10^{16} \text{ cm}^{-3}$ , the loss rate values at 0.8 K and 0.2 K drawn from Fig. 6b are about  $2 \times 10^{-19} \text{ cm}^3/\text{ns}$  and  $10^{-19} \text{ cm}^3/\text{ns}$ , respectively, which are an order of magnitude less than those reported in refs. 12 and 13. Presumably, inhomogeneity of the strain field introduces some addition.

Returning to Fig. 5a, one sees that for  $S > S_0$  paraexcitons have  $a < 0$  corresponding to an effective attractive interaction. BEC of a trapped Bose gas with  $a < 0$  is possible,<sup>45–47</sup> but unstable leading to the condensate's collapse.<sup>48–50</sup> This happens when the number of condensate particles  $N_0$  exceeds a critic number  $N_{cr} \approx 0.46 a_{ho}/|a|$  ( $a_{ho}$  – the mean harmonic oscillator length). For the trap with  $a_{ho} \approx 0.615 \mu\text{m}$  under  $S = 1.4$  kbar (corresponding to  $a \approx -0.295 \text{ nm}$ ) from ref. 10,  $N_{cr} \approx 960$ . Probably, that this number was exceeded in the condensate the authors achieved, so it collapsed and subsequently exploded. To avoid this, stress  $S \leq S_0$  ensuring nonnegative  $a$  must be used. Let us consider the limit of strong interaction  $N_0 a/a_{ho} \gg 1$ , wherein the condensate radius increases with  $N_0$ ,  $R \approx a_{ho}(15N_0 a/a_{ho})^{1/5}$ .<sup>45</sup> It is reasonable to take a value of  $S$  in the

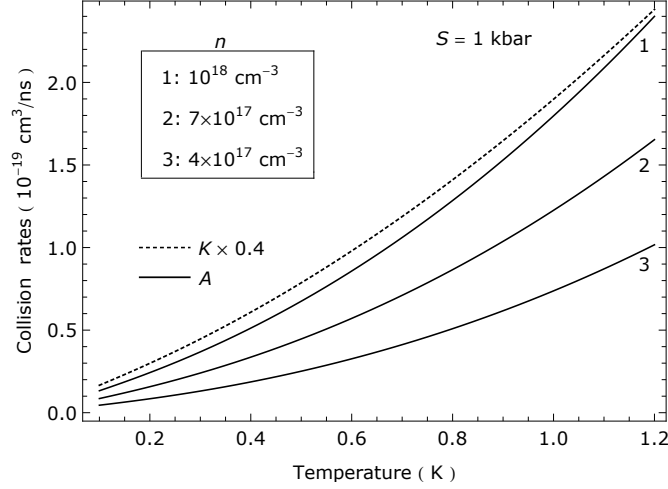


Figure 7: **Temperature dependence of the paraexciton elastic collision rate and loss rate at high densities.** Taking the trap from ref. 10 with  $2 \times 10^9$  paraexcitons, the density of  $10^{18} \text{ cm}^{-3}$ ,  $7 \times 10^{17} \text{ cm}^{-3}$  and  $4 \times 10^{17} \text{ cm}^{-3}$  corresponds to the condensation fraction 12%, 5% and 1%, respectively.

vicinity of  $S_0$ , when the decay and loss parameters have their minimum, say 1 kbar corresponding to  $a \approx 0.018 \text{ nm}$ . Then for the trap from ref. 10,  $a/a_{ho} \approx 3 \times 10^{-5}$ . Let  $N_0$  be as high as  $2 \times 10^8$  yielding  $N_0 a/a_{ho} \approx 6 \times 10^3$  and  $R \approx 6 \mu\text{m}$ , which corresponds to  $n = N_0/R^3 \approx 9 \times 10^{17} \text{ cm}^{-3}$ . From Fig. 7 we find, that at 0.8 K and  $n = 10^{18} \text{ cm}^{-3}$ ,  $A \approx 1.3 \times 10^{-19} \text{ cm}^3/\text{ns}$ . Inhomogeneous broadening might somewhat raise the value, but explosion due to small  $a$  is excluded. We note in passing, that domination of the elastic collision rate over loss rate remains even for such a high density. Thus, a stable paraexciton condensate might take place under experimental conditions of ref. 10 provided the applied stress  $S \leq S_0$ .

## Discussion

It is the analogy of excitons with atoms that has motivated the search for BEC in  $\text{Cu}_2\text{O}$ . However, the distinguishing feature is that excitons are composite entities made from charge-carriers – fermions, whose Coulomb-mediated correlations are governed by the Pauli exclusion principle. The internal structure of excitons produces the spin-dependent exciton-exciton interaction that governs their BEC. In the case of yellow-series 1s excitons in  $\text{Cu}_2\text{O}$ , it results in the interconversion between a pair of paraexcitons with mutual repulsive interaction and that of orthoexcitons, which attract each other, leading to the two-channel character of the paraexciton-paraexciton scattering. We have described the scattering at low temperature in the approximation of coupled bare channels accepted in scattering theory. By an approximate way of calculating the nonlocal exchange exciton-exciton interaction potential, we have been able to estimate the paraexciton background scattering length  $a_{bg}$ , binding energy  $\mathcal{E}_b$  of a biexciton supported by the closed channel as well as strength  $\Gamma_c$  of the coupling between the biexciton and paraexciton scattering states. The coupling

makes the biexciton a Feshbach resonance with its two characteristic effects – a loss of particles in the open channels and a diminution of their background scattering length, which give us clues about the mechanism of obstacles to paraexciton BEC. First, the loss of paraexcitons observed in numerous experiments is elucidated, which turns out to be connected with continued conversion of two paraexcitons into the quasibiexciton as an intermediate state. Reflecting the paraexciton decaying nature characteristic of semiconductor electronic excitations, the loss rate is proportional to the paraexciton decay width, which comprises of the exciton-exciton and exciton-phonon scattering widths and also inhomogeneous broadening. The last explains divergence of measurements of the loss rate in different experiments. At relatively high temperatures, when exciton-phonon scattering is effective and rises with temperature, the rate can be high. In an unstressed crystal, it is likely the main reason of the paraexciton saturation at high densities. However, of our interest in this paper are strain-confined paraexcitons at temperatures near one Kelvin and below. By shifting paraexciton and orthoexciton energies in different ways, stress reduces the ortho-para splitting and by this enhances quasibiexciton effects. We have found that, although the component related to the exciton-exciton scattering increases with stress, steep decrease of exciton-phonon scattering rate at such low temperatures makes the paraexciton loss inefficient to affect BEC. Collisional properties of paraexcitons is then determined solely by their scattering length  $a$ , which is affected by the other quasibiexciton effect. At an applied stress  $S_0$ , the background scattering length is balanced by the diminution induced by the quasibiexciton, so  $a = 0$ , then it turns negative for  $S > S_0$ . Our rough numerical estimates give  $S_0$  of order of one kilobar. Thus we have revealed that already moderate stress, which is generally used to produce potential traps for paraexcitons to prevent their diffusion as well as to lower their critical density, makes the paraexciton scattering length negative. As BEC of trapped bosons with  $a < 0$  is unstable leading to the condensate's collapse, this creates a serious obstacle to attaining a convincing BEC. This result is supported by the process of ‘explosion’ of paraexcitons under stress of 1.4 kbar below the critical temperature seen by Gonokami's group.

Our quantitative estimates, in particular that of the critical value  $S_0$  of applied stress, have relied on three parameters  $a_{bg}$ ,  $\mathcal{E}_b$  and  $\Gamma_c$  computed by using approximate exchange interaction potential. The potential shape is sensitive to  $\beta$ , which is rather uncertain in connection with some discrepancy in measurements of exciton key parameters  $E_b$ ,  $a_x$  and  $\mu_x$ . A slight modification of  $\beta$  can lead to considerable variations of  $\mathcal{E}_b$  and  $\Gamma_c$ , and consequently, changes the value of  $S_0$ . But that is not the whole picture. The approximation of two coupled bare channels applied in this paper is a good one for scattering energy  $E \ll 2\Delta$ . However, its disadvantage lies in the estimate of the coupling strength  $\Gamma_c$ , which has been obtained from the second-order correction to the quasibiexciton energy produced by the coupling potential as a perturbation. That was a rough approximation because the exchange exciton-exciton interaction potential is not weak. The perturbation caused by this potential to quasistates of bare channels seems more complicated. In this context, our treatment gives just general qualitative features of collisional properties of cold paraexcitons leaving much room for quantitative improvement by experiments as well as by other theoretical approaches.

## Acknowledgements

The author would like to thank M. Kuwata-Gonokami and K. Yoshioka for valuable discussions, wherein initial ideas for this work were formed, and S. A. Moskalenko and Nguyen Thanh Phuc for critical reading of the manuscript. The financial support from Vietnam National Foundation for Science and Technology Development (NAFOSTED) through Grant No. 103.01-2014.73 is acknowledged.

## References

- [1] Moskalenko, S. A. Reversible optico-hydrodynamic phenomena in a nonideal exciton gas. *Fiz. Tverd. Tela.* **4**, 276–284 (1962); *Sov. Phys. Solid State* **4**, 199–204 (1962).
- [2] Blatt, J. M., Böer, K. W. & Brandt, W. Bose–Einstein condensation of excitons. *Phys. Rev.* **126**, 1691–1692 (1962).
- [3] Keldysh, L. V. & Kozlov, A. N. Collective properties of excitons in semiconductors. *Zh. Eksp. Teor. Fiz.* **54**, 978–993 (1968); *Sov. Phys. JETP* **27**, 521–528 (1968).
- [4] Agekyan, V. T. Spectroscopic properties of semiconductor crystals with direct forbidden energy gap. *Phys. Status Solidi A* **43**, 11–42 (1977).
- [5] Mysyrowicz, A., Hulin, D. & Antonetti, A. Long exciton lifetime in Cu<sub>2</sub>O. *Phys. Rev. Lett.* **43**, 1123–1126 (1979).
- [6] Hulin, D., Mysyrowicz, A., & Benoit a la Guillaume, C. Evidence for Bose–Einstein statistics in an exciton gas. *Phys. Rev. Lett.* **45**, 1970–1973 (1980).
- [7] Trauernicht, D. P. , Wolfe, J. P. & Mysyrowicz, A. Thermodynamics of strain-confined paraexcitons in Cu<sub>2</sub>O. *Phys. Rev. B* **34**, 2561–2575 (1986).
- [8] Snoke, D.W., Wolfe, J. P. & Mysyrowicz, A. Evidence for Bose–Einstein condensation of a two-component exciton gas. *Phys. Rev. Lett.* **64**, 2543–2546 (1990).
- [9] Lin, J. L. & Wolfe, J. P. Bose–Einstein condensation of paraexcitons in stressed Cu<sub>2</sub>O. *Phys. Rev. Lett.* **71**, 1222–1225 (1993).
- [10] Yoshioka, K., Chae, E. & Kuwata-Gonokami, M. Transition to a Bose–Einstein condensate and relaxation explosion of excitons at sub-Kelvin temperatures. *Nature Commun.* **2**, 328 (2011).
- [11] Yoshioka, K. & Kuwata-Gonokami, M. Relaxation explosion of a quantum degenerate exciton gas in Cu<sub>2</sub>O. *New J. Phys.* **14**, 055024 (2012).
- [12] Schwartz, R., Naka, N., Kieseling, F. & Stolz, H. Dynamics of excitons in a potential trap at ultra-low temperatures: paraexcitons in Cu<sub>2</sub>O. *New J. Phys.* **14**, 023054 (2012).
- [13] Stolz, H. et al. Condensation of excitons in Cu<sub>2</sub>O at ultracold temperatures: experiment and theory. *New J. Phys.* **14**, 105007 (2012).

- [14] Snoke, D. & Kavoulakis, G. M. Bose–Einstein condensation of excitons in  $\text{Cu}_2\text{O}$ : progress over 30 years. *Rep. Prog. Phys.* **77**, 116501 (2014).
- [15] O’Hara, K. E., Suilleabhain, L. O. & Wolfe, J. P. Strong nonradiative recombination of excitons in  $\text{Cu}_2\text{O}$  and its impact on Bose–Einstein statistics. *Phys. Rev. B* **60**, 10565–10568 (1999).
- [16] Denev, S. & Snoke, D. W. Stress dependence of exciton relaxation processes in  $\text{Cu}_2\text{O}$ . *Phys. Rev. B* **65**, 085211 (2002).
- [17] Yoshioka, K., Ideguchi, T., Mysyrowicz, A. & Kuwata-Gonokami, M. Quantum inelastic collisions between paraexcitons in  $\text{Cu}_2\text{O}$ . *Phys. Rev. B* **82**, 041201R (2010).
- [18] Kavoulakis, G. M. & Baym, G. Auger decay of degenerate and Bose-condensed excitons in  $\text{Cu}_2\text{O}$ . *Phys. Rev. B* **54**, 16625–16636 (1996).
- [19] Jang, J. I. & Wolfe, J. P. Auger recombination and biexcitons in  $\text{Cu}_2\text{O}$ : A case for dark excitonic matter. *Phys. Rev. B* **74**, 045211 (2006).
- [20] Wolfe, J. P. & Jang, J. I. The search for Bose–Einstein condensation of excitons in  $\text{Cu}_2\text{O}$ : exciton-Auger recombination versus biexciton formation. *New J. Phys.* **16**, 123048 (2014).
- [21] Landau, L. D. & Lifshitz, E. M. *Quantum Mechanics* Chs. XII, XVII, XVIII (Pergamon, New York, 1985).
- [22] Koster, G. F., Dimmock, J. O., Wheeler, R. G. & Statz, H. *Properties of the Thirty-two Point Groups* (MIT, Cambridge, 1963).
- [23] Hanamura, E. Theory of the high density exciton. I. *J. Phys. Soc. Japan* **29**, 50–57 (1970).
- [24] Hanamura, E. Theory of many Wannier excitons. I. *J. Phys. Soc. Japan* **37**, 1545–1552 (1974).
- [25] Bobrysheva, A. I., Miglei, M. F. & Shmiglyuk, M. I. On the bi-exciton formation in crystals. *Phys. Status Solidi B* **53**, 71–84 (1972).
- [26] Nguyen Ba An, Hoang Ngoc Cam, and Nguyen Trung Dan. Spin-dependent exciton-exciton interaction potential in two- and three-dimensional semiconductors under excitation. *J. Phys.: Condens. Matter* **3**, 3317–3329 (1991).
- [27] Hoang Ngoc Cam. Exciton and biexciton nonlinearities in coherent four-wave mixing in semiconductor quantum wells. *Zh. Eksp. Teor. Fiz.* **129**, 315–335 (2006); *Russian JETP* **102**, 277–296 (2006).
- [28] Hoang Ngoc Cam. Biexciton-biexciton interaction in semiconductors. *Phys. Rev. B* **55**, 10487–10497 (1997).
- [29] Heitler, W. & London, F. Interaction between neutral atoms and homopolar binding according to quantum mechanics. *Z. Phys.* **44**, 455–472 (1927).



- [30] Kotani, M., Ohno, K. & Kayama K. in *Encyclopedia of Physics*, Vol. XXXVII/2, Molecule, II (ed Flugge S.) 1–172 (Springer Verlag, Berlin, 1961).
- [31] Kavoulakis, G. M., Chang, Y. C. & Baym, G. Fine structure of excitons in  $\text{Cu}_2\text{O}$ . *Phys. Rev. B* **55**, 7593–7599 (1997).
- [32] Frohlich, D., Brandt, J., Sandfort, C., Bayer, M. & Stolz, H. Anisotropic effective mass of orthoexcitons in  $\text{Cu}_2\text{O}$ . *Phys. Rev. B* **84**, 193205 (2011).
- [33] Shumway, J. & Ceperley, D. M. Quantum Monte Carlo treatment of elastic exciton-exciton scattering. *Phys. Rev. B* **63**, 165209 (2001).
- [34] Brinkman, W. F., Rice, T. M. & Bell, B. The excitonic molecule. *Phys. Rev. B* **8**, 1570–1580 (1973).
- [35] Huang, W. T. Binding energy of excitonic molecules in isotropic semiconductors. *Phys. Status Solidi B* **60**, 309–317 (1973).
- [36] Coz, M., Arnold, L. G. & MacKellar A. D. Nonlocal potentials and their local equivalents. *Ann. Phys.* **59**, 219–247 (1970).
- [37] Taylor, J. R. *Scattering theory: The quantum theory on nonrelativistic collisions* (John Wiley & Sons, New York, 1972). Chs. 12, 20.
- [38] Feshbach, H. A unified theory of nuclear reactions. II. *Ann. Phys.* **19**, 287–313 (1962).
- [39] Cheng Chin, Grimm, R., Julienne, P. & Tiesinga, E. Feshbach resonances in ultracold gases. *Rev. Mod. Phys.* **82**, 1225–1286 (2010).
- [40] Waters, R. G., Pollack, F. H., Bruce, R. H. & Cummins, H. Z. Effects of uniaxial stress on excitons in  $\text{Cu}_2\text{O}$ . *Phys. Rev. B* **21**, 1665–1675 (1980).
- [41] Trauernicht, D. P. & Wolfe, J. P. Drift and diffusion of paraexcitons in  $\text{Cu}_2\text{O}$ : Deformation-potential scattering in the low-temperature regime. *Phys. Rev. B* **33**, 8506–8521 (1986).
- [42] Sobkowiak, S., Semkat, D. & Stolz, H. Modeling of the thermalization of trapped paraexcitons in  $\text{Cu}_2\text{O}$  at ultralow temperatures. *Phys. Rev. B* **90**, 075206 (2014).
- [43] Brandt, J. et al. Ultranarrow optical absorption and two-phonon excitation spectroscopy of  $\text{Cu}_2\text{O}$  paraexcitons in a high magnetic field. *Phys. Rev. Lett.* **99**, 217403 (2007).
- [44] Tiesinga, E., Moerdijk, A. J., Verhaar, B. J. & Stoof, H. T. C. Conditions for Bose-Einstein condensation in magnetically trapped atomic cesium. *Phys. Rev. A* **46**, R1167–R1170 (1992).
- [45] Dalfovo, F., Giorgini, S., Pitaevskii, L. P. & Stringari, S. Theory of Bose-Einstein condensation in trapped gases. *Rev. Mod. Phys.* **71**, 463–512 (1999).
- [46] Bradley, C. C., Sackett, C. A., Tollett, J. J. & Hulet, R. G. Evidence of Bose-Einstein condensation in an atomic gas with attractive interactions. *Phys. Rev. Lett.* **75**, 1687–1690 (1995).

- [47] Bradley, C. C., Sackett, C. A. & Hulet, R. G. Bose-Einstein condensation of lithium: observation of limited condensate number. *Phys. Rev. Lett.* **78**, 985–988 (1997).
- [48] Ruprecht, P. A., Holland, M. J., Burnett, K., & Edwards, M. Time-dependent solution of the nonlinear Schrodinger equation for Bose-condensed trapped neutral atoms. *Phys. Rev. A* **51**, 4704–4711 (1995).
- [49] Roberts, J. L. et al. Controlled collapse of a Bose-Einstein condensate. *Phys. Rev. Lett.* **86**, 4211–4214 (2001).
- [50] Donley, E. A. et al. Dynamics of collapsing and exploding Bose–Einstein condensates. *Nature* **412**, 295–299 (2001).